

Differential Source Count for Gamma Ray Bursts

SHREYA BANERJEE,¹ DAVID EICHLER,² AND DAFNE GUETTA³

¹*Inst. for Quantum Gravity, FAU Erlangen-Nuremberg, Staudtstr. 7, 91058 Erlangen, Germany*

²*Department of Physics, Ben-Gurion University, P.O.Box 653, Beer-Sheva 84105 Israel*

³*Department of Physics, ORT-Braude College, Karmiel, Israel*

ABSTRACT

The logN-logF distribution for a certain classes of intrinsic luminosity functions (ILF) is considered. It is found that the best fit ILF is in good agreement with the ILF predicted in the companion paper (Banerjee et al 2020) which is based on an explicit physical model. The results are consistent with the observation of a comparable number of flat phase afterglows and monotonic decreasing ones.

Keywords: gamma-ray burst: general

1. INTRODUCTION

GRBs are among the brightest cosmological explosions in the universe, mostly lasting from a few seconds to a few thousand seconds. GRBs could be useful tools to investigate high redshift objects.

An intrinsic luminosity function (ILF) is among the most sought after quantities for any class of astrophysical objects. From quasars to various types of galaxies to supernovae, etc., these distributions provide important insights not only into the physics of the individual objects themselves, but also into the evolution of matter in our universe.

For GRBs, which are believed to be beamed along a jet axis, the intrinsic luminosity function also sheds light on the angular emission profile of the GRB, assuming the observers are distributed isotropically. As only a small, possibly biased fraction of GRBs have observed redshifts at the present time, the derivation of their luminosity function has presented a difficult problem, especially at the low luminosity end. In particular, it is not settled whether low L emission along lines of sight well of the jet axis is dominated by a) material moving at angular offset to the line of sight, or b) by material moving along the line of sight. If these photons would be moving backward, moving more than $1/\Gamma$ from the emitting material in the observer's frame or in the frame of the presumably ultra-relativistic emitting material, this would have enormous implications for models of GRBs, where it is frequently assumed that the observed emission is beamed *forward*.

A luminosity function is a measure of the number of objects per unit luminosity and therefore is intimately connected to the energy budget (e.g., mass and rotational energy) and the physical parameters determining the emission mechanism (e.g. density and magnetic field) of the objects.

Because GRBs are most likely associated with some sort of compact object(s) (e.g., a very massive star, or two compact objects, such as neutron stars or black holes, merging), getting a handle on the GRB luminosity function and event rate could have important consequences for understanding not only GRBs themselves, but other astrophysical problems as well.

There exists an inevitable scatter in intrinsic luminosities of the GRBs, it is not clear if this scatter is due to relativistic beaming as offset viewers may see diminished luminosity. Scatter in the intrinsic luminosity can cause a selection bias. When the scatter in luminosity is strong, it is important to quantify the effect to distinguish it from true dynamical evolution. Thus, it is important to study luminosity selection effects in GRBs in order to identify

Corresponding author: Shreya Banerjee

shreya.banerjee@fau.de

eichler.david@gmail.com

dafnaguetta@braude.ac.il

the bias. In our earlier work (Banerjee et al 2020), we studied the intrinsic luminosity function (ILF) using a test on median luminosity.

To date, several authors, such as in (Guetta and Piran 2005, Guetta and Piran 2007, Guetta et al 2005, Guo et al 2020, Firmani et al 2005, Tsvetkova et al 2017, Petrosian et al 2015, Pescalli et al 2016, Guetta and Piran 2006), have tried to constrain the luminosity function from the observed fluxes of GRB. Most of these papers consider a broken power law luminosity function, $N(L) \propto (L/L_0)^{-\alpha}$ for $L < L_0$ and, $N(L) \propto (L/L_0)^{-\beta}$ for $L > L_0$, and give constraints on the low and high power law index and on the luminosity break. In paper1 we have considered different choices of the luminosity function parameters and tested them with the median luminosity method. We find results that are consistent with what found by previous authors within their uncertainties (Pescalli et al 2016).

In this paper, we attempt to constrain the ILF $N(L)$, using the observed $N(F)$, i.e. the numbers of GRBs observed per unit flux interval. Assuming that GRBs follow the star formation rate (Lloyd-Ronning et al 2002, Yonetoku et al 2004), for each $N(L)$, it is possible to find the implied $N(F)$ and compare it to the observed data. The paper is organized as follows: in Section 2 we describe our physical model and the choices of the luminosity function forms, in Section 3 we describe the method used to constrain the luminosity function parameters, in Section 4 we present our results and conclusions.

2. DESCRIPTION OF THE PHYSICAL MODEL AND METHODOLOGY

We consider a class of physical models presented in paper1. For simplicity we consider a uniform jet where the prompt GRB emission is in a beam (“pencil” beam). We assume that all the jets are identical, i.e. with the same Lorentz factor Γ and opening angle θ_0 . We also assume that the distribution of observers is isotropic. They would nevertheless be distributed in intrinsic luminosities L because different observers would see them at different viewing angles. For GRBs observed slightly off the edge of the jet, the source should be considered extended. In this case the luminosity function can be represented by a power law $N(L)dL \propto L^{-\alpha}dL$ with a power law index $\alpha = 1.33$ near the edge of the jet and $\alpha = 1.25$ far from the jet (Eichler 2004, Banerjee et al 2020). In order to test the models in paper1 we employed a statistical test based on median luminosity. We considered that GRBs have a power law distribution function $N(L)dL \propto L^{-\alpha}dL$ where α corresponds to the spectral index whose value lies between $1 < \alpha < 2$. We tested values of $\alpha = 5/4$ and $\alpha = 4/3$ which corresponds to the cases when the prompt GRB emission is in a narrow “pencil” beam and GRBs observed slightly off the edge of the jet (extended source) respectively. We have also tested the case of an optically thin jet and found that it cannot explain the data because it predicts too many bright jets in comparison to what is observed. When the shell is optically thick, observers outside the jet see the same LF as the observers outside an optically thin shell because they are seeing photons that are scattered backwards in the frame of the shell. However observers within the opening angle of the jet cannot see photons backscattered from material moving directly at them. Therefore there is a “blind spot”. These observers see backscattered photons only from jet material outside the blind spot. The calculation of the blind spot size, θ_{BS} , is outlined in (Eichler 2014). It shows that the minimum angle of the blind spot depends on the optical depth of the shell and on the distribution of circumburst material. The blind spot means that there is a minimum offset between the observed material and the line of sight. This is in contrast to observers outside the jet who can come arbitrarily close to the edge of the jet. If the illumination is in pulses the observers within the jet see a light echo from those parts of the jet that are outside the blind spot. Most of the time integrated signal comes from an annulus just outside the blind spot and comparable in solid angle to the solid angle of the blind spot itself. If the observer is well within the jet the annulus completely surrounds the blind spot, but if the blind spot touches the edge of the jet then the annulus is only partial and the observer very close to the edge of the jet sees an annulus that it is only about half of the circle. The geometry of this model is discussed in detail in (Vyas, Peers and Eichler 2021). For observers just outside the jet the luminosity function can be represented by a power law as described above. For observers inside the jet the luminosity function depends on the distribution of blind spot sizes. If the distribution is scale free then it is reasonable to represent this by another power law (if the blind spot size is bigger than the jet opening angle then it become meaningless because the emission the observers see is identically zero). The total luminosity function is then the sum of the luminosity functions for observers outside the jet and the ones inside the jet. So we always write the ILF as the sum of two terms, $N(L) = N_{in}(L) + N_{out}(L)$. The $N_{out}(L)$ is a power law as discussed above. If the distribution of the a blind spot sizes is scale free, then it is reasonable to represent $N(L)_{in}$ as a different power law. In this case, the total ILF can be approximately represented by a broken power law $N(L) \propto (L/L_0)^{-\alpha}$ for $L < L_0$ and, $N(L) \propto (L/L_0)^{-\beta}$ for $L > L_0$. If the blind spot has a characteristic scale (the opposite extreme is scale free) i.e. $\theta_{BS} \sim 3/\Gamma$ as estimated in Eichler 2014, then the $N_{in}(L)$ should be dominated

by a peak at the corresponding luminosity. In this case, the total ILF can be represented by the sum of a power law and a delta function $N(L) \propto \delta(L - L_{\text{break}})$.

In this paper we consider the two possible ILF forms described above and test these models against observed *flux* distributions. The novelty of this paper is based on the fact that we are trying to fit observed data using a ILF based on a possible physical interpretation of the GRBs LF. In order to to constraint our model parameters we use the Fermi GBM sample of GRBs, thereby finding the physical model that explains the data most accurately.

3. DIFFERENTIAL COUNT

Let $N(L, z)$ be the luminosity distribution function of a class of emitters: the rate of detected GRBs per unit comoving volume per unit luminosity at a redshift z .

The number of GRBs or the event rate (in short, the source count) with observed peak flux greater than F is then given by

$$N(> F) = \int_0^{z_{\text{max}}} dz' \frac{dV}{dz'} \frac{1}{(1+z')} \int_{L_{\text{min}}}^{L_{\text{max}}} dL' N(L', z') \quad (1)$$

Here, V is the comoving volume, z_{max} is the upper bound on the redshift and L_{min} is the luminosity derived from the threshold flux of the detector at given redshift. The factor $(1+z')^{-1}$ is included to account for the time dilation of the interval between detected bursts.

L_{min} can be written as

$$L_{\text{min}} = 4\pi D_L^2(z) F \quad (2)$$

where D_L is the luminosity distance whose form depends on the choice of the cosmological model.

dV/dz is the comoving volume element per unit of redshift, and is given by

$$\frac{dV}{dz'} = \frac{4\pi D_L^2(z')}{(1+z')} \frac{dt}{dz'} \quad (3)$$

where t is the cosmic time.

For a Friedman universe,

$$\frac{dz}{dt} = -(1+z)H(z) = -(1+z)H_0(\Omega_m(1+z)^3 + \Omega_\Lambda)^{1/2} \quad (4)$$

where $H(z)$ is the Hubble parameter, Ω_{m0} , $\Omega_{\Lambda0}$ and H_0 are the present values of matter density, cosmological constant and Hubble parameter respectively.

In order to fit Eq. 1 with data, we will be considering the Λ CDM model.

Following the analysis and results of (Banerjee et al 2020), we consider the power law form of the luminosity function considered in our previous work.

The local luminosity function of GRB peak luminosities L , defined as the comoving space density of GRBs in the interval L to $L + dL$, is

$$\mathcal{N}(L) = c_0 \left(\frac{L}{L_{\text{max}}} \right)^{-\alpha} \quad (5)$$

where c_0 is a normalization constant with dimension of $1/L$ so that the integral over the luminosity function equals unity.

Considering the evolution of the luminosity function with redshift such that $N(L, z) = N(L)N(z)$ (as in (Lloyd-Ronning et al 2002, Yonetoku et al 2004)), we get

$$N(L, z) = \rho_0 c_0 \left(\frac{L}{L_{\text{max}}} \right)^{-\alpha} (1+z)^k = N_0 \left(\frac{L}{L_{\text{max}}} \right)^{-\alpha} (1+z)^k \quad (6)$$

out to some maximum redshift z_{max} , beyond which N is assumed to vanish. ρ_0 is the GRB rate at $z = 0$ expressed in units of $Gpc^{-3}year^{-1}$, N_0 is the normalization constant that needs to be fixed. Here α is the spectral index with $1 < \alpha < 2$ and k is the new parameter that determines the dependency on the redshift z . The condition $1 < \alpha < 2$ implies that while most of the power is in the brightest sources, there are more dim sources than bright ones. The evolution of the luminosity function is determined by the parameter k .

In order to fix the normalization constant, we integrate Eq. 6 over L and z . Choosing the value of $k = 1.4$ from (Lloyd-Ronning et al 2002, Yonetoku et al 2004) and considering $z_{max} = 10$ appropriate for star formations, we get the rate of GRBs as 2 per day for $\rho_0 \approx 5.5 Gpc^{-3} yr^{-1}$, consistent with that observed by Swift/GBM.

Substituting the above definitions in Eq. 1 and performing the integral over L we get

$$N(> F) = N_0 L_{max}^\alpha \int_0^{z_{max}} dz' \frac{4\pi D_L^2(z')(1+z')^k}{(\alpha-1)H_0(1+z')^3(\Omega_m(1+z')^3 + \Omega_\Lambda)^{1/2}} (L_{max}^{-\alpha+1} - (4\pi D_L^2(z')F)^{-\alpha+1}) \quad (7)$$

Data Sample: In order to constrain the model, we need to compare our expectations with the data. For our present analysis, we will consider the observed data from (Gruber et al 2014, Kienlin et al 2014, Bhat et al 2016). Our sample consists of 918 short and long GRBs detected by Fermi Gamma Ray Bursts monitor. The sample consists of the peak flux distributions of these GRBs as detected by Fermi GBM. We then obtained the histogram representing the event rate per unit flux interval i.e. the differential source count by dividing the 918 bursts in the GBM catalog into 135 bins of equal size according to their value of the peak flux.

In order to compare with data, we consider the differential count, $dN(> F)/dF$ defined as \mathcal{N} , of Eq. 7. The corresponding expression is given by

$$|\mathcal{N}| = N_0 L_{max}^\alpha F^{-\alpha} \int_0^{z_{max}} dz' \frac{(4\pi D_L^2(z'))^{-\alpha+2}(1+z')^k}{H_0(1+z')^3(\Omega_m(1+z')^3 + \Omega_\Lambda)^{1/2}} \quad (8)$$

The normalization constant N_0 is fixed by the value of the local GRB rate as explained earlier. One can also express N_0 in terms of the model parameters and then fix it by assuming the model curves to match the observed data at value of $\mathcal{N} = 2.2$ corresponding to the highest value (brightest GRB) of F present in the observed sample. For the present sample, this corresponds to setting $\mathcal{N} = 2.2$ at $F = 1 \times 10^{-5}$ i.e. all the curves match the data at the highest available energy/flux. Here and henceforth L_{max} is in units of erg/s and F is in units of erg/cm²/s.

Thus the expression for N_0 , in terms of the model parameters, turns out to be

$$N_0 = \frac{2.2}{L_{max}^\alpha \left[F^{-\alpha} \int_0^{z_{max}} dz' \frac{(4\pi D_L^2(z'))^{-\alpha+2}(1+z')^k}{H_0(1+z')^3(\Omega_m(1+z')^3 + \Omega_\Lambda)^{1/2}} \right]_{F=10^{-5}}} \quad (9)$$

From Eq. 8 and Eq. 9, we see that the theoretical predictions are independent of uncertainties in the true z_{max} and k , depend just on α . All the curves will coincide for any reasonable value of z_{max} and k . However, while choosing the value of z_{max} , one needs to keep in mind that the condition $L_{max} \geq 4\pi D_L^2 F$ should always be satisfied for the entire range of F for which we are obtaining the differential count.

In Fig. 1, we have plotted the variation of \mathcal{N} with F for $\alpha = 1.5, 1.33, 1.25, 1.17$ (which are the standard values used in our earlier paper (Banerjee et al 2020)). These curves represent all the values of z_{max} lower than its value mentioned in the preceding paragraph.

We have further considered the case when ILF is the sum of two ILF as described in Section 2. In this case the ILF can be approximated by a broken power law-

$$N(L) \propto (L/L_0)^{-\alpha}, \quad L < L_0 \quad (10)$$

$$\propto (L/L_0)^{-\beta}, \quad L > L_0 \quad (11)$$

We consider different values for α, β, L_0 and looked for the combination that fits the data most accurately. Using this ILF we plot the $\log N - \log F$ distribution in Fig. 1.

In order to compare the theoretical models corresponding to different values of α we use the method of χ^2 minimization and p value. The level of significance is a predefined threshold, which in our case has been set as 0.05. The results have been shown in Table 1. From Table 1, we can see that $\alpha = 1.33$ has the lowest χ^2 value of 0.069 with the p value equal to 0.79. The broken power law with $\alpha = 1.3, \beta = 1.8, L_0 = 10^{51}$ (Pescalli et al 2016) lies close by with the corresponding values $\chi^2 = 0.12, p = 0.73$. In Table 1, we have mentioned the results of other combinations of (α, β, L_0) . As we can see, we get the best fit for $\alpha = 1.5, \beta = 1.33, L_0 = 5 \times 10^{51}$ with χ^2 value of 0.072 and p value equal to 0.8. We have also shown certain other combinations of the parameter values which do not give good fit and hence are rejected. For example, for $\alpha = 1.6, \beta = 1.1, L_0 = 5 \times 10^{50}$, the p value is 0.65. $\alpha = 1.25$ with $\chi^2 = 0.12, p = 0.73$ do not give the best fit, but is still not ruled out by the present sample. Comparing the χ^2 and

p-values, we see that for simple power law, $\alpha = 1.33$ fits the data most closely with the broken power law lying close by and for broken power law, we get the best fit for $\alpha = 1.5$, $\beta = 1.33$, $L_0 = 5 \times 10^{51}$. Our results are consistent with the results found by (Pescalli et al 2016), where $\alpha \sim 1.3$ (for $L < L_0$) and $\beta \sim 1.8$ (for $L > L_0$) and a break luminosity $L_0 = 10^{51}$ erg/sec.

An interesting information is the ratio between the observers outside the jet and the ones inside. This can be estimated by convolving the, $N(L)_{\text{in}}$ and $N(L)_{\text{out}}$, with observed volume as explained in Eq. 1.

For the best fit values obtained earlier i.e. for $\alpha = 1.5$, $\beta = 1.33$, $L_0 = 5 \times 10^{51}$, this ratio is 1.2. Thus we see that with these parameter values, the observed GRBs are almost equally distributed outside and inside the jet.

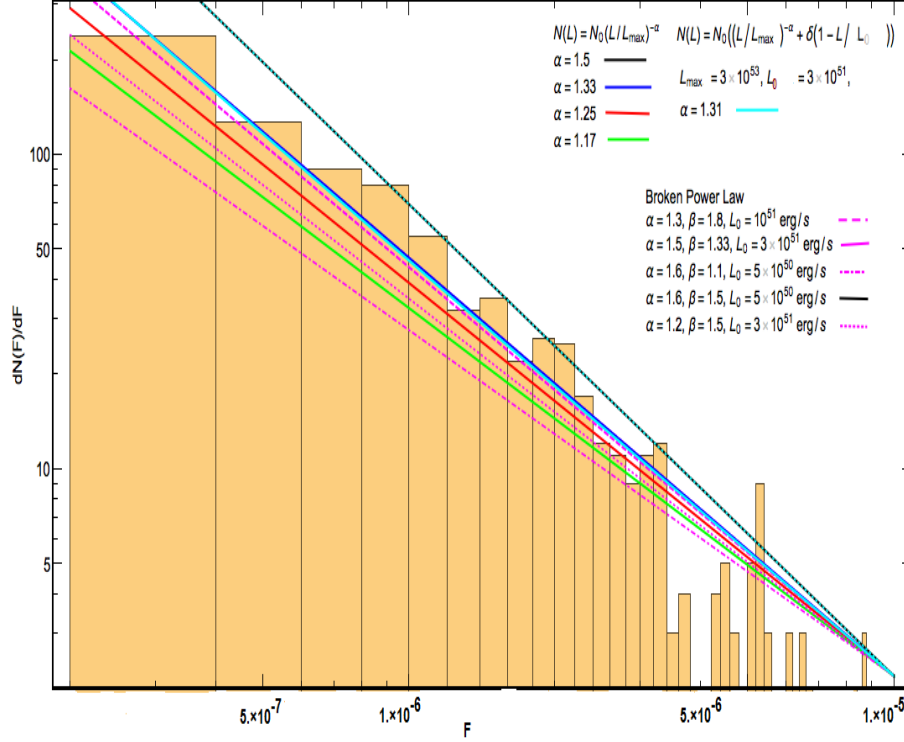


Figure 1. Variation of \mathcal{N} with F for single power law and broken power law. Single power law: Black curve- $\alpha = 1.5$, blue curve- $\alpha = 1.33$, red curve- $\alpha = 1.25$, green curve- $\alpha = 1.17$. Broken power law-($\alpha = 1.3$, $\beta = 1.8$, $L_0 = 1 \times 10^{51}$)-dashed magenta curve, ($\alpha = 1.5$, $\beta = 1.33$, $L_0 = 3 \times 10^{51}$)-solid magenta curve, ($\alpha = 1.6$, $\beta = 1.1$, $L_0 = 5 \times 10^{50}$)-dot-dashed magenta curve, ($\alpha = 1.6$, $\beta = 1.5$, $L_0 = 5 \times 10^{50}$)-black magenta curve, ($\alpha = 1.2$, $\beta = 1.5$, $L_0 = 3 \times 10^{51}$)-dotted magenta curve. Delta function plus single power law-($\alpha = 1.31$, $L_{\text{max}} = 3 \times 10^{53}$, $L_0 = 3 \times 10^{51}$)-cyan curve. Data is given by the histogram.

We also consider the case when $N(L, z)$ is a sum of a power law and a delta function around L_{max} . The luminosity function is now given by

$$N(L, z) = N_0 \left(\left(\frac{L}{L_{\text{max}}} \right)^{-\alpha} + \delta \left(1 - \frac{L}{L_0} \right) (1+z)^k \right) \quad (12)$$

The delta function represents the contribution of jets of finite solid angle observed head on.

The source count is now given by

$$\begin{aligned} N(> F) = & N_0 \int_0^{z_{\text{max}}} dz' \frac{L_0(1+z)^k}{F H_0(1+z)^3 (\Omega_m(1+z)^3 + \Omega_\Lambda)^{1/2}} \\ & + N_0 L_{\text{max}}^\alpha \int_0^{z_{\text{max}}} dz' \frac{4\pi D_L^2(z')(1+z')^k}{(\alpha-1) H_0(1+z')^3 (\Omega_m(1+z')^3 + \Omega_\Lambda)^{1/2}} (L_{\text{max}}^{-\alpha+1} - (4\pi D_L^2(z')F)^{-\alpha+1}) \end{aligned} \quad (13)$$

α	χ^2	p-value
1.17	0.225	0.64
1.25	0.12	0.73
1.33	0.069	0.79
1.5	0.126	0.72
$\alpha = 1.3, \beta = 1.8, L_0 = 1 \times 10^{51}$	0.12	0.73
$\alpha = 1.5, \beta = 1.33, L_0 = 3 \times 10^{51}$	0.072	0.8
$\alpha = 1.6, \beta = 1.1, L_0 = 5 \times 10^{50}$	0.21	0.65
$\alpha = 1.6, \beta = 1.5, L_0 = 5 \times 10^{50}$	0.126	0.72
$\alpha = 1.2, \beta = 1.5, L_0 = 3 \times 10^{51}$	0.18	0.65
$\alpha = 1.31, L_{max} = 3 \times 10^{53}, L_0 = 3 \times 10^{51}$	0.072	0.8

Table 1. Table containing the χ^2 and p values for single, broken power laws and single power law with delta function.

The corresponding expression for differential source count is

$$\begin{aligned}
|\mathcal{N}| = & N_0 L_{max1}^\alpha F^{-\alpha} \int_0^{z_{max}} dz' \frac{(4\pi D_L^2(z'))^{-\alpha+2} (1+z')^k}{H_0(1+z')^3 (\Omega_m(1+z')^3 + \Omega_\Lambda)^{1/2}} \\
& + N_0 F^{-2} \int_0^{z_{max}} dz' \frac{L_{max2}(1+z)^k}{H_0(1+z)^3 (\Omega_m(1+z)^3 + \Omega_\Lambda)^{1/2}}
\end{aligned} \tag{14}$$

Setting $\mathcal{N} = 2.2$ at $F = 1 \times 10^{-5}$, we get the expression for N_0 as

$$N_0 = \frac{2.2}{\left[L_{max1}^\alpha F^{-\alpha} \int_0^{z_{max}} dz' \frac{(4\pi D_L^2(z'))^{-\alpha+2} (1+z')^k}{H_0(1+z')^3 (\Omega_m(1+z')^3 + \Omega_\Lambda)^{1/2}} + F^{-2} \int_0^{z_{max}} dz' \frac{L_{max2}(1+z)^k}{H_0(1+z)^3 (\Omega_m(1+z)^3 + \Omega_\Lambda)^{1/2}} \right]_{F=1 \times 10^{-5}}} \tag{15}$$

In Fig. 1, we have shown the curve that best fit the data for a delta function around the best fit value of the break luminosity obtained earlier. For the present case, the best fit curve is obtained for $\alpha = 1.31$, $L_{max} = 3 \times 10^{53}$, $L_0 = 3 \times 10^{51}$. The corresponding χ^2 and p values have been shown in Table 1.

4. CONCLUSION

In this paper, we studied the behaviour of the differential source count \mathcal{N} for a given luminosity function as a companion paper of paper1 (Banerjee et al 2020) and compared it with the flux distribution of Fermi GBM data. In our present work, we have chosen a class of physical models described in (Eichler 2014 and references therein). This model is basically a shell with a baryonic material illuminated from behind possibly optically thick. For simplicity we have considered a constant bulk Lorentz factor and an opening angle θ_0 . The GRB Intrinsic Luminosity Function (ILF) consists of a contribution of $N_{out}(L)$ observers outside the jet and $N_{in}(L)$ inside θ_0 . $N_{out}(L)$ has been calculated in paper1 and can be approximated as $N(L)dL \propto L^{-\alpha}dL$ where $\alpha = 4/3$ for observers just outside the jet and $\alpha = 5/4$ for observers far from the jet. This power law extends to a maximum value that corresponds to the observers within $1/\Gamma$ of the edge of the jet. For observers inside the jet, $N_{in}(L)$ depends on the distribution of blind spot sizes because the optical depth is large when the shell is illuminated from behind. In this case the blind spot hides material within it. It was argued in Eichler 2014 that the blind spots size is likely to be larger than $1/\Gamma$. Therefore the brightest bursts may well be dominated by $N_{out}(L)$ and possibly some optically thin bursts. If $N_{in}(L)$ is represented by a power law, then it should be softer more biased to lower luminosities and have a steeper power law index. If at the other extreme the blind spots have all the same size then $N_{in}(L)$ is represented by a delta function that peaks at a luminosity much less than the maximum luminosity. As it is difficult to know the distribution of blind spot sizes, we considered both extremes. We find very similar results for the p-values of the best fit of the broken power law and the power law with the delta function implying that the logN-logF distribution is insensitive to the distribution of the blind spot sizes. We find that the best fit ILF is in good agreement with the values of α calculated in paper1 and with values found in the literature. The number of observed bursts from outside the GRB jets is comparable to the number of the GRB jets observed within the GRB angle. This is quite consistent with the observation that the number of GRBs with flat

phase afterglow is comparable to the number of GRBs with monotonic decreasing afterglow and the hypothesis that the observers outside the jet see flat phase afterglow while those inside the jet see monotonic decreasing afterglow.

We conclude that the physical model is consistent with both observational tests discussed in paper1 and in this paper.

5. DATA AVAILABILITY

The data underlying this article are available in the article and can be found in (Gruber et al 2014, Kienlin et al 2014, Bhat et al 2016).

6. ACKNOWLEDGEMENTS

We would like to thank with Avishai Gal-Yam, Richard Ellis, Elena Pian and Paolo Mazzali for useful discussions. We acknowledge funding from Israel Science Foundation and John and Robert Arnow Chair of Theoretical Astrophysics.

REFERENCES

- Banerjee, S., Eichler, D., and Guetta, D., arXiv:2010.04810.
- Bhat, P. N., *et al.*, 2016, ApJ. Supplement series, **223**, 2.
- Firmani, C., Avila-Reese, V., Ghisellini, G., Tutukov, A. V., 2005, NCimC, **28**, 4.
- Goldstein, A., Veres, P., Burns, E., *et al.*, 2017, ApJL, doi:10.3847/2041-8213/aa8f41.
- Guetta, D., and Piran, T., 2005, A&A, **435**, 421-426.
- Guetta, D., Piran, T., A&A, 2006, **453**, 3.
- Guetta, D., and Piran, T., 2007, JCAP, **07**,003.
- Guetta, D., Piran T. and Waxman, E., 2005, ApJ, **619**, 412-419.
- Gruber, D., *et al.*, 2014, ApJ. Supplement series, **211**, 1.
- Guo, Qi., *et al.*, 2020, ApJ, **896**, 1.
- Kienlin, A. V., *et al.*, 2014, ApJ. Supplement series, **211**, 1.
- LIGO Scientific Collaboration & Virgo Collaboration, 2017a, GCN, **21505**, 1; LIGO Scientific Collaboration & Virgo Collaboration, 2017b, GCN, **21513**, 1; LIGO Scientific Collaboration & Virgo Collaboration, 2017c, GCN, **21527**, 1.
- Lloyd-Ronning, N., *et al.*, 2002, ApJ, **574**, 554–565.
- Pescalli, A., *et al.*, 2016, A&A, **587**, A40.
- Petrosian, V., Kitanidis, E., Kocevski, D., ApJ, 2015, **806**, 44.
- Savchenko, V., Ferrigno, C., Kuulkers, E., *et al.*, 2017b, ApJL, 999.
- Tsvetkova, A., *et al.*, ApJ, 2017, **850**, 161.
- Yonetoku, D., *et al.*, 2004, ApJ, **609**, 935.
- Vyas, M. K, Peer, A., Eichler, D. 2021, arXiv:2011.02973